AAEC/E331

AAEC/E331

AUSTRALIAN ATOMIC ENERGY COMMISSION

RESEARCH ESTABLISHMENT

LUCAS HEIGHTS

THE MEASUREMENT OF SWIRLING FLOW IN HIFAR FUEL ELEMENTS AND THE EFFECTS OF FITTING FLOWSPLITTERS

by

J. MARSHALL

January 1975

ISBN 0 642 99668 7

AUSTRALIAN ATOMIC ENERGY COMMISSION
RESEARCH ESTABLISHMENT
LUCAS HEIGHTS

THE MEASUREMENT OF SWIRLING FLOW IN HIFAR FUEL ELEMENTS AND THE EFFECTS OF FITTING FLOWSPLITTERS

by

J. MARSHALL

ABSTRACT

Measurements have been made of swirl in the coolant flow at the inlet of HIFAR fuel elements before and after flowsplitters were fitted in the inlet nozzles. There was considerable swirl before installation of the flowsplitters, and the amplitudes and directions of the swirl formed a symmetrical pattern over the core. The swirl activity distribution appears to have a definite relationship to positions in which some fuel element damage had been noticed.

After flowsplitters were fitted, the swirl velocities were found to have been reduced by a factor of about twenty.

National Library of Australia card number and ISBN 0 642 99668 7

The following descriptors have been selected from the INIS Thesaurus to describe the subject content of this report for information retrieval purposes. For further details please refer to IAEA–INIS–12 (INIS: Manual for Indexing) and IAEA–INIS–13 (INIS: Thesaurus) published in Vienna by the International Atomic Energy Agency.

COOLANTS; FUEL ELEMENTS; FLOW REGULATORS; HIFAR REACTOR; LIQUID FLOW; NOZZLES; TURBULENT FLOW; VELOCITY; VORTEX FLOW; VORTICES

CONTENTS

(continued)

CONTENTS (Continued)

1. INTRODUCTION

Difficulties have been experienced in the DIDO/PLUTO type reactors owing to failure of the Mark 4 fuel elements. This problem was thought to be due partly to the occurrence of strong vortex swirls in the flow at the inlet of the fuel element support nozzles (K.K. George, UKAEA unpublished report). Similar problems in the reactor HIFAR have led to vibration experiments on fuel elements (Gleed 1973), attempts to measure vibration conditions (Harris & Holland 1974), and eventually to proposals for the installation of flowsplitters or straighteners within the inlet nozzles (Figure 1). Similar devices have been used in the British reactors PLUTO and DIDO and in the Danish reactor DR3 with beneficial results to fuel element and rig life. In HIFAR (and in DR3) the flowsplitters are designed as separate solid vane assemblies having an interference fit in the support nozzles. They are fitted by being cooled in a liquid nitrogen bath and then inserted rapidly into position, thus being locked in place owing to the interference fit created on expansion to normal temperature.

The experiments reported here were carried out to investigate the existence or otherwise of swirling flow at the fuel element inlets in HIFAR, and to compare conditions existing before the installation of the flowsplitters with conditions created afterwards. The experiments involved design and construction of a rig, including a special purpose vorticity meter suitable for measurement of swirl in the coolant flow at each of the fuel element inlet nozzles.

2. MEASUREMENT EQUIPMENT

2.1 Location and General Design

Figure 2 shows the position of the measuring device in the reactor HIFAR. A turbine with straight, axially aligned blades (the vorticity meter) is located at the end of a liner which fits inside the Mark 4 fuel element. The turbine blades are arranged in this way so as to measure only the swirling component of flow, and are positioned as near as possible to the point where the flow leaves the fuel element inlet nozzle. More detail of this positioning is shown in Figure 3, which also shows the guide shield. This latter component is required to facilitate feed to the liner through the fuel element and the fuel plate support combs. The guide shield has a taper inlet and circumferential webs, which together are designed not only to support the liner against the combs during insertion, but also to give minimum interference with the coolant flow when fully installed. These features may be seen more clearly in Figure 4.

The complete instrumented liner for rig X189 is shown in diagrammatic form in Figure 5, and a cross-section of the vorticity meter is shown in Figure 6. Figure 7 shows the leads wound around the lifting bolt after being fed through a helical hole in the shield plug.

2.2 Vorticity Meter

The turbine blades are integral with the bearing-tube. This assembly rotates on graphite-to-steel bearings. The graphite sleeves are a push fit into the tube. The stationary component of the bearings is formed by the central stainless steel shaft. Stainless steel thrust pads are provided at the top and bottom ends of the bearing tube. It is considered that the large flow generally causes a net upwards thrust during operation, but the turbine could operate with reversed thrust if necessary. During assembly, the tube fitted with bearings was put over the spindle and then the lower pad and locknut were adjusted to obtain suitable fit conditions. The end cap and vanes were then fitted and spot-welded. This method of construction was used to enclose the bearings and thus minimise the possibility of debris or broken parts being released into the reactor.

To detect rotation of the turbine, permanent magnet bars are held in the fixed steel transition block with wire coils wound directly over them. Mild steel plugs of diameter 0.125" (~ 3 mm) are fixed at 120° intervals around the turbine end, and as these pass over the magnet faces the changing flux pattern causes voltage to be generated in the coils. There are two magnets, spaced 150° apart, and by comparing the time of signals, it is possible to determine the direction of rotation. The interval between pulses from one magnet and coil determines the rotation speed of the turbine, there being three pulses per revolution. The signal is taken *via* a stainless steel sheathed, two-wire mineral-insulated lead to a connector at the top of the liner end shield plug. It is a fully insulated signal suitable for input to conventional differential amplifiers to give good pickup noise rejection performance.

2.3 Recording System

A diagram of the instrumentation and recording system is given in Figure 8. Leads from the amplifiers to the magnet coils were made *via* the connectors on the liner top. These leads had to be fed downwards through the reactor top plate (Figure 2) each time the liner was installed in a new position. It was important to maintain constant lead connections throughout the experiment and, since the connectors were interchangeable, the leads and connectors were colour coded. The leads were also fitted with handles designed to facilitate

fitting at a distance; they were also designed to foul against the lifting bolt if they were not correctly installed.

3. MEASUREMENTS MADE BEFORE FITTING THE FLOWSPLITTERS

3.1 Experimental Procedure and Derivation of Data

Measurements in this condition were made during two consecutive reactor shutdown periods (1-2 May and 28-29 May 1973) and covered all 25 fuel element positions, each having three combinations of pump pairs. Records were taken of the signals for about four minutes in each condition.

During the first experimental period the signals were recorded on magnetic tape and then replayed later on to a high speed chart recorder for analysis. In the second period the high speed chart recorder was also taken to the reactor so that signal samples could be taken simultaneously with the recording. Analysis of the signals consisted of the visual examination of the charts to count samples of pulses and to compare the phase of the two signals. A list of results is given in Table 1. Gaps are left in the table where the particular quantity seems inappropriate, *e.g.* in the low activity channels it is often not possible to state with certainty whether the turbine has a net rotation in any direction; it is also not appropriate to derive a value for maximum activity. These difficulties are illustrated by the samples of typical signals given in Figures 9, 10, 11 and 12. The signals from the channels varied considerably in amplitude and frequency and, for convenience, the results have been categorised into four levels of activity:

Category	Average Pulse Rate (pulse s^{-1})
1	> 20
2	10-20
3	5-10
4	< 5

The sample from channel A2 (Figure 9) shows that the signal has a high pulse rate. It appears to be rotating at a variable speed but at all times in a clockwise direction with bursts of speed rising to over 60 pulse s^{-1} (equivalent to 20 rev s^{-1}). The mean pulse rate is about 30 pulse s^{-1} and so this is a category 1 channel. The signals show clearly the characteristic pulse pattern as the mild steel plug passes over the magnet and coil. The phase difference between the two signals, with the peak of the RED signal occurring just before the peak of the GREEN signal, indicates that RED is

leading and, therefore, the turbine is rotating clockwise looking from the reactor top.

Figure 10 shows a category 2 channel in which the GREEN signal leads the RED, indicating anticlockwise rotation. Position C3 (see Figure 11) apparently has a tendency to oscillate; some parts of the signal have the GREEN channel leading whereas other parts have the RED channel leading. This is a category 3 channel with mean pulse rate about 6 pulse s^{-1}.

An example of a low activity category 4 channel, position D4, is shown in Figure 12. The pulses appear infrequently and at spasmodic intervals. Here, it was not possible to determine definitely if there was any constant rotational direction because of the scarcity of pulse pairs, *i.e.* pulses from the two channels occurring closely in time.

Figure 13 shows the results of a pump changeover in which pump 1 was switched off and then pump 2 was switched on. The pulse rate first decays and then rises.

Table 1 summarises all the results and gives the category of each condition. The results are also displayed in Figure 14 on a plan of the reactor core. This indicates the distribution of the various rotational activity levels around the core, and the direction of rotation at each location.

Figure 15 shows the statistical distribution of pulse period for each of the pump combinations of channel A2. These were obtained by an automatic signal analysis system in which the time between each zero crossing of the signal was measured and stored for a 20-second length of signal. It can be seen that the mean pulse frequency, *i.e.* the total number of pulses divided by the total time, agrees well with the manual measurements in Table 1. The distributions for the three pump combinations differ slightly but all have the peak at about 23 ms and have the same skew shape with a tail at the long period end, and a sharp cut-off point below 17 ms. The counts at around one millisecond are probably due to noise on the signal.

3.2 Interpretation of Results

3.2.1 Accuracy of measurement

The results presented in Table 1 are relatively simple to interpret. A2 is by far the most active location tested and there is strong net rotation in the clockwise direction. Location D4 is relatively very inactive in the rotational component of flow. However, in deriving the absolute levels of rotational velocity, the characteristics of the turbine are very significant. The most important parameters are:

- The bearing friction characteristics.
- The time response.

These are discussed in more detail in Appendices A and B respectively; broadly speaking, the first parameter tends to limit the lowest speed of swirl to which the turbine will respond, and the second tends to result in failure to measure high speed short duration bursts of swirl. The lowest swirl response speed is estimated as about 0.1 rev s^{-1}, based upon static friction levels, and the time response is shown to be that of a simple time constant of about 3 ms. Therefore, it is considered that the turbine is likely to have revealed any fluid rotation of practical interest and also that the shortest bursts (see Figure 6) are most probably indicative of actual fluid conditions.

3.2.2 Distribution pattern

The distribution of rotational activities displayed in Figure 14 shows considerable symmetry in both rate and direction of rotation when considered relative to a vertical line through the centre position C3. The two halves are almost mirror images. This symmetry extends even to the centre channel C3, which is split by this line and which exhibits an oscillatory tendency by appearing to have bursts of both clockwise and anticlockwise movement. Differences are shown in the rates of activity of A1 and A2 relative to A3 and A4, and in B3 relative to B4. The latter case is fairly marginal with B3 being just within the higher rank, in fact one pump combination is actually within the lower rank. A2 is by far the most active channel and thus something of an anomaly. No particular reason can be seen for its high activity relative to A3.

3.2.3 Postulated plenum chamber flow pattern

A plenum chamber flow pattern which might give rise to the swirl directions is illustrated in Figure 16. The fluid flowing from the risers will be guided by the narrowing outer circumference of the plenum chamber and to some extent by support stubs. Flow from separate risers will interact and the overall flow pattern may well be somewhat similar to that shown. The axis of symmetry aligns with the position of the risers and it is possible to postulate a completely symmetrical flow pattern to concur with the measured swirl directions.

3.2.4 Different pump combinations

Table 1 also lists the effect of different pump combinations at each position. From this it will be seen that there are differences, but these are small compared to the differences between channels. The differences

appear relatively larger in the channels with low activity, but this is probably due to the errors in estimating the pulse rates in these channels rather than to real differences. At low pulse rates (see Figures 11 and 12), it is often difficult to decide what constitutes a pulse and this uncertainty contributes to the scatter in the tabulated results.

The statistical distributions of pulse periods given in Figure 16 for position A2 at different pump combinations show some differences but, as already mentioned, the general features are very similar.

4. MEASUREMENTS MADE AFTER FITTING THE FLOWSPLITTERS

4.1 Experimental Procedure

This part of the experiment was carried out over two periods. The first tests took place during the reactor shutdown period (25-27 August 1973) immediately after the fitting of flowsplitters. A further series of tests were performed about six months later, on 5 February 1974. The procedure and equipment were essentially the same as those described in Section 2. The rig was slightly contaminated at the end of the previous tests and had to be kept in a storage facility for about three months prior to the August 1973 tests. Some deterioration had occurred during this storage period (see Appendix B) resulting in high starting torque, and it was felt desirable to confirm the earlier results; this was done during the February 1974 tests when rather more activity was indicated than in the August tests on channel A2 but not on the other channels.

Results from all post-flowsplitter tests are given in Table 2. Owing to shortage of time, tests were made on only nine fuel element positions. These included the previous most active channel A2 and others chosen because of previous histories and geometrical distributions. Positive results were only possible on channels A2 and A3, all other positions being too low in rotational activity for the present instrument to measure.

5. DISCUSSION

The tests were made because fuel damage had occurred in overseas reactors of the DIDI/PLUTO type, and also in HIFAR. It is of interest, therefore, to compare the results obtained here against results from fuel element vibration tests carried out at the AAEC Research Establishment (Harris & Holland 1974) and also the HIFAR fuel damage experience summarised in Appendix C.

A comparison between vibration levels measured by Harris & Holland and the swirl and the fuel damage experienced (H. Moeskops, AAEC unpublished report) is given in Figure 17. It can be seen that the relationship between

vibration and swirl was not as strong as might have been expected. Some positions, such as B4 and B5, had high level vibration in both of Harris & Holland's measurements (*i.e.* as measured by accelerometers at the bottom of the liner, and also as measured at the reactor top on the shield plug), but the swirl level was very low. There was also a moderate amount of swirl in all the E row positions but a minimum of vibration. The worst swirl position was, however, a high vibration position.

There appears to be a fair degree of correlation between the swirl and damage. In Appendix C it can be seen that the worst position is A2 where one fuel element was severely damaged and there was a contribution to bad damage in another. The main anomaly in the damage list is at position C5 which is a very low activity swirl position. However, it will be noted that this particular fuel element spent only one program in C5 and five in E4, so C5 may in fact have contributed very little to the damage. Similarly, although B4 had to be marked as a high damage position, the fuel element had also been in position A2, and this could have been the prime damage generator.

After the flowsplitters were fitted, the rotational activity was considerably reduced, as can be seen by comparing Table 2 with Table 1. Channel A2 changed from about 10 rev s^{-1} to around 0.5 rev s^{-1} and actually changed direction of swirl. This reversal of swirl direction in A2 was quite unexpected and may indicate that a completely new flow pattern is now present in the plenum chamber. Channel A3 also reduced by about the same factor but the direction remained unchanged.

6. CONCLUSIONS

The experiments clearly demonstrated the presence of swirl flow in HIFAR fuel element inlet nozzles before the fitting of flowsplitters. The swirl flow appears to be consistent with a postulated flow pattern distribution within the plenum chamber, taking into account the relative spacing of inlet risers, circumferential walls, support stubs and fuel element nozzles. Channel A2 had swirl rising to at least 20 rev s^{-1} for durations of the order of 100 to 300 ms; the swirl in channels A3, A4, B3, C2 and C4 was about half that in channel A2. The channels B1, B2, B5, B6, C1, C5, D3 and D4 had relatively low swirl activity.

Fitting the flowsplitters caused a dramatic change in the swirl activity. The previously strong swirl pattern appears to have been destroyed, even to the extent of reversing the direction of swirl in the previously most active position. Any swirl remaining is at low velocity and below the level at

which the present instrument can measure with reliability.

7. ACKNOWLEDGEMENTS

The project was initiated by Dr. T.J. Ledwidge (now at the Darling Downs Institute of Advanced Education, Toowoomba, Queensland) who also helped in various design decisions. All the mechanical items were made by Mr. V. Cornford who also contributed largely in the mechanical design and in conducting the experiments. Considerable cooperation was given by all Reactor Operation Section staff and particularly by the Active Handling Group in the many reactor top operations.

8. REFERENCES

Harris, R.W. & Holland, P.G.(1974) - Results of vibration scan of HIFAR reactor core positions using the instrumented liner X184. AAEC/E337

Gleed, D.B. (1973) - A review of some recent vibration experiments on materials testing reactor fuel elements. AAEC/TM635.

Schenk, K. (1967) - Turbine flowmeter for in-core applications. OECD Halden Reactor Project. Report HPR72.

Sabersky, R.A., Acosta, A.J. & Hauptmann, E.G. (1971) - Fluid Flow. Macmillan, London.

TABLE 1

RESULTS BEFORE FITTING THE FLOWSPLITTERS

Fuel Element	Pumps	Tape	Position	Gain	Activity			Mean Rotation (rev s^{-1})	Lead Signal	Direction	Rank
					Maximum pulse s^{-1}	Minimum pulse s^{-1}	Average pulse s^{-1}				
A1	1 & 2	6	610	200	25		5		R	C	3
	1 & 3	6	660	500	23		6		R	C	3
	2 & 3	6	700	500	23		6		R	C	3
A2	1 & 2	43	48	200	60	12	33	11	R	C	1
	1 & 3	43	120	200	52	10	28	9	R	C	1
	2 & 3	43	170	200	55	12	32	10	R	C	1
A3	1 & 2	43	642	500	33	4	12	4	G	A	2
	1 & 3	43	665	500	32		14	5			
	1 & 3	6	880	500							4
	2 & 3	6	920	500	8		3				4
D4	1 & 2	41	448	1,000							4
	1 & 3	41	470	1,000							4
	2 & 3	41	480	1,000					R	C	3
D5	1 & 2	41	22	500			5		R	C	3
	1 & 3	41	73	500			7		R	C	3
	2 & 3	41	106	500			6		R	C	3
D6	1 & 2	41	165	500	23		9		R	C	3
	1 & 3	41	230	500	23		8		R	C	3
	2 & 3	41	253	500			7		G	A	3
E1	1 & 2	43	826	500	33		8		G	A	2
	1 & 3	43	876	500	27		10		G	A	3
	2 & 3	43	903	500			7		R	C	3
E2	1 & 2	41	320	500			5		R	C	3
	1 & 3										3
	2 & 3	41	403	1,000			6				4
E3	1 & 2	43	932	500			5				3
	1 & 3	43	960	500			4				3
	2 & 3	43	982	500			5		R	C	3
E4	1 & 2	6	950	200	25		8		R	C	3
	1 & 3	6	990	200	35		9		R	C	3
	2 & 3	6	1,010	200	31		8				

C Clockwise
A Anticlockwise
} *Looking down from the reactor top.*

G Green

R Red

TABLE 2

SUMMARY OF RESULTS AFTER FITTING THE FLOWSPLITTERS

Fuel Element	Pulse Burst Rate (pulse s^{-1})		Rotation Speed (rev s^{-1})		Direction
	August	February	August	February	
A2	0.35	1.6	0.1	0.53	Anticlockwise
A3	0.5	0.3	0.16	0.1	Anticlockwise
B2	-		-		-
B3	-		-		Clockwise
B4	-		-		-
C2	-		-		-
C3	-		-		-
C4	-		-		-
E1	-		-		-

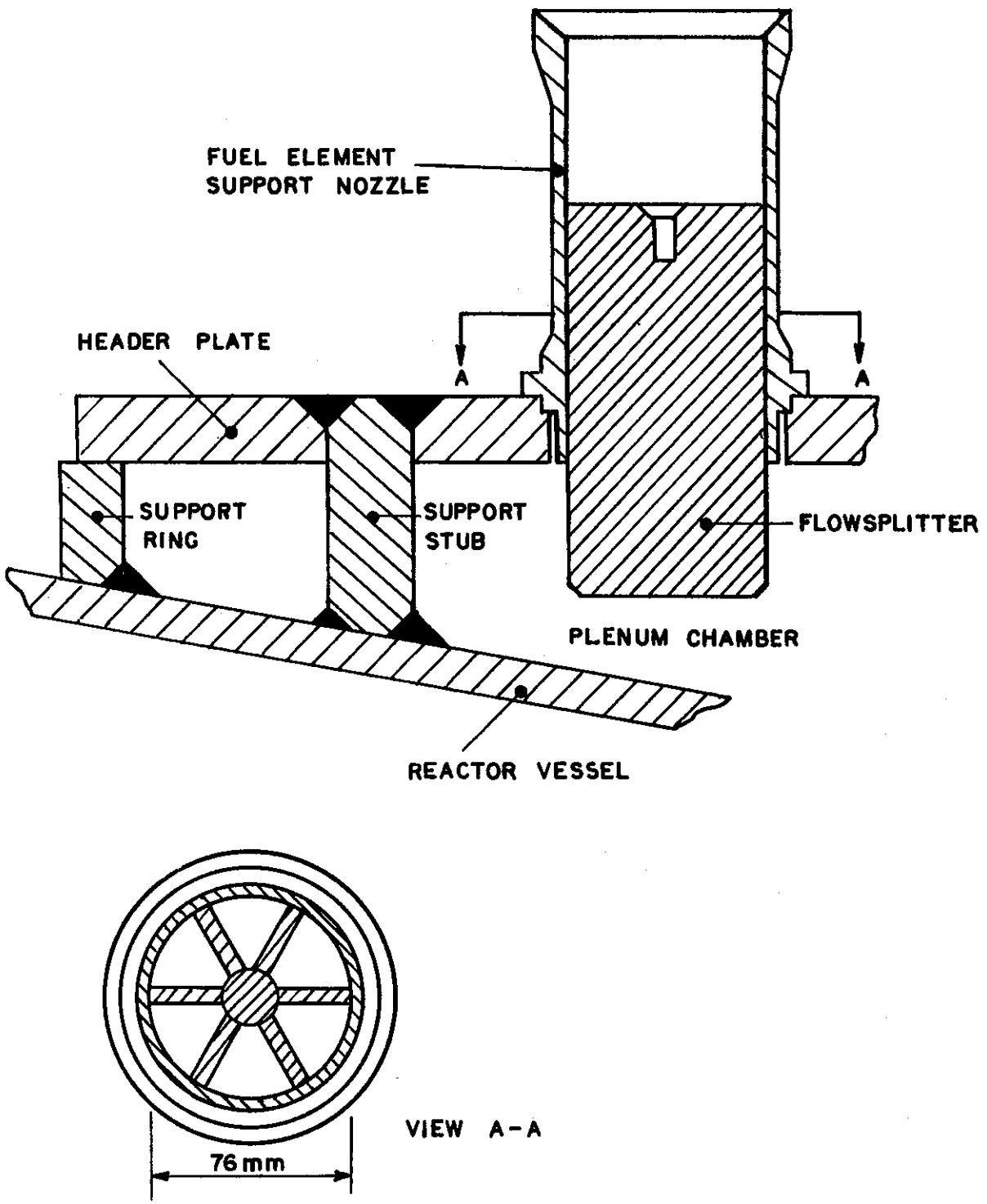

FIGURE 1. FLOWSPLITTER ARRANGEMENT

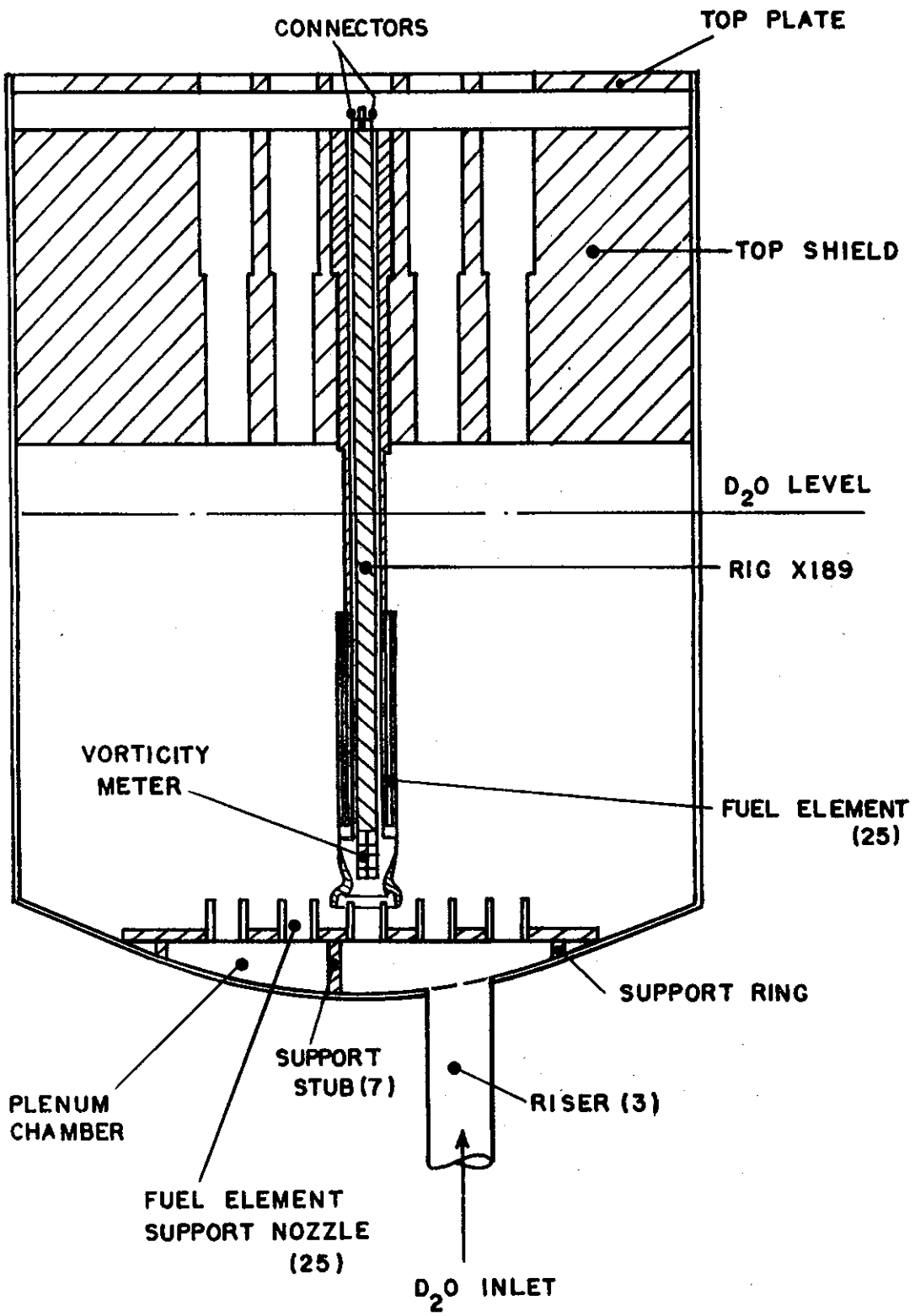

FIGURE 2. HIFAR - POSITION OF THE VORTICITY METER IN THE CORE

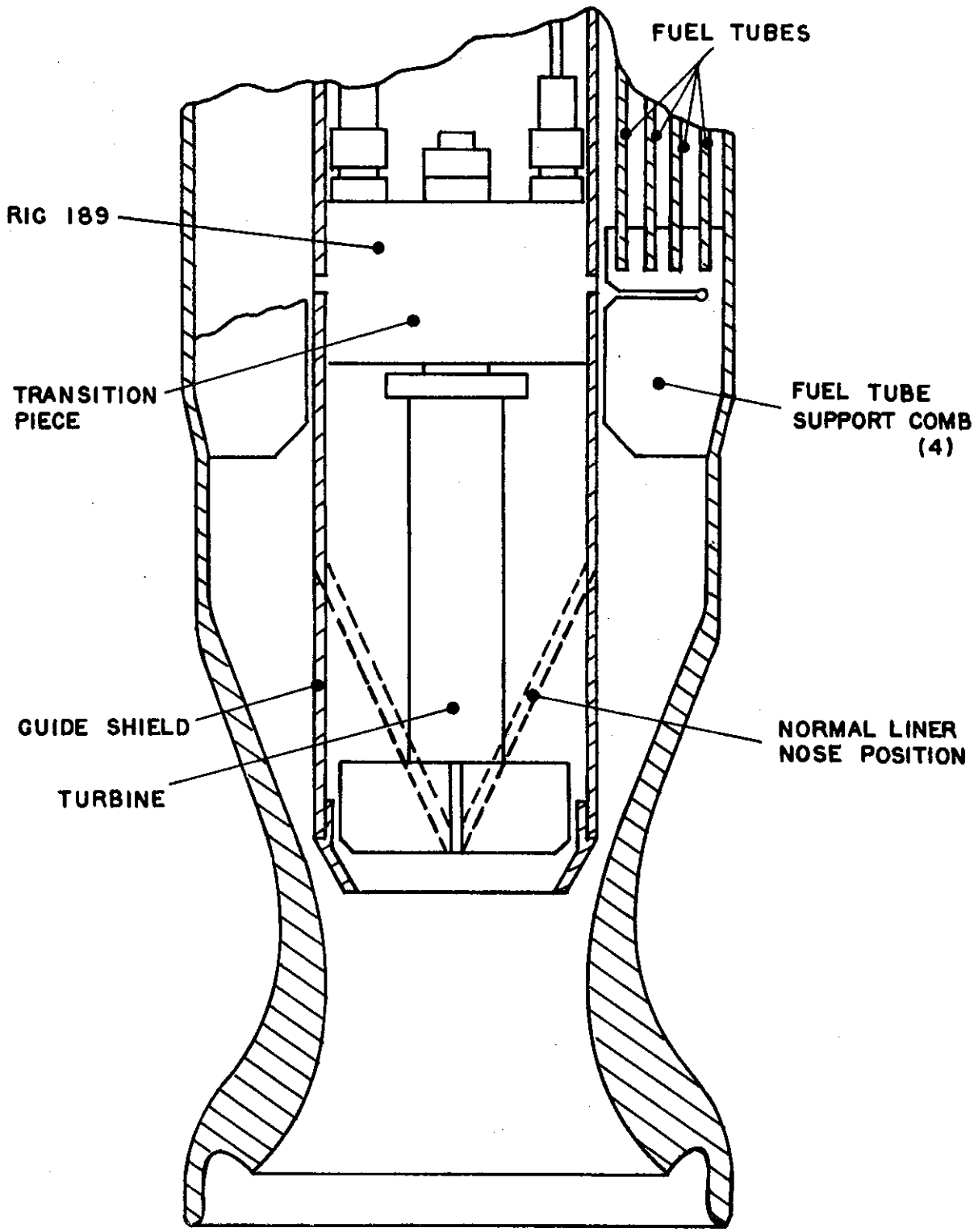

FIGURE 3. POSITION OF THE VORTICITY METER IN THE FUEL ELEMENT

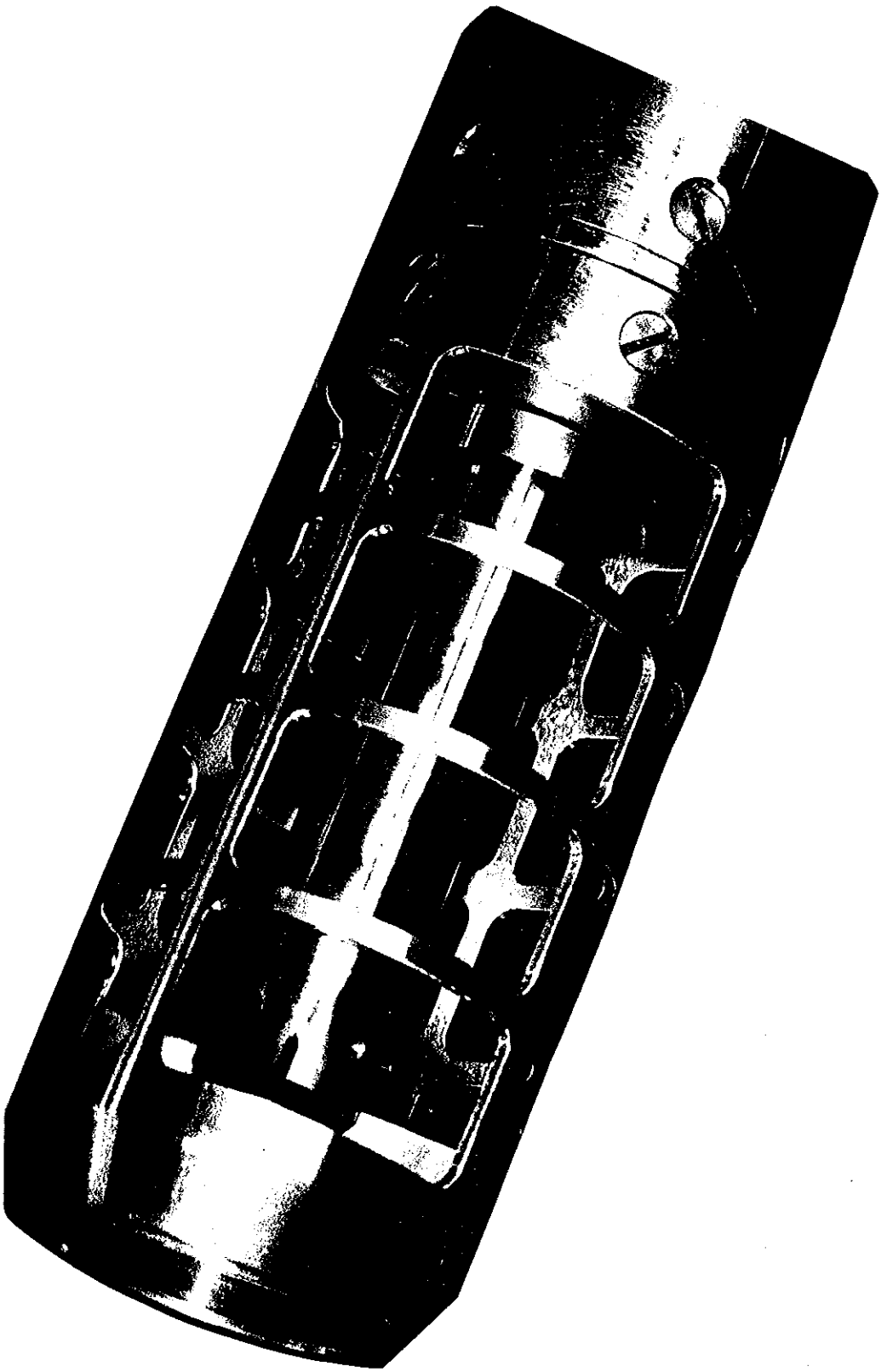

FIGURE 4. VORTICITY METER

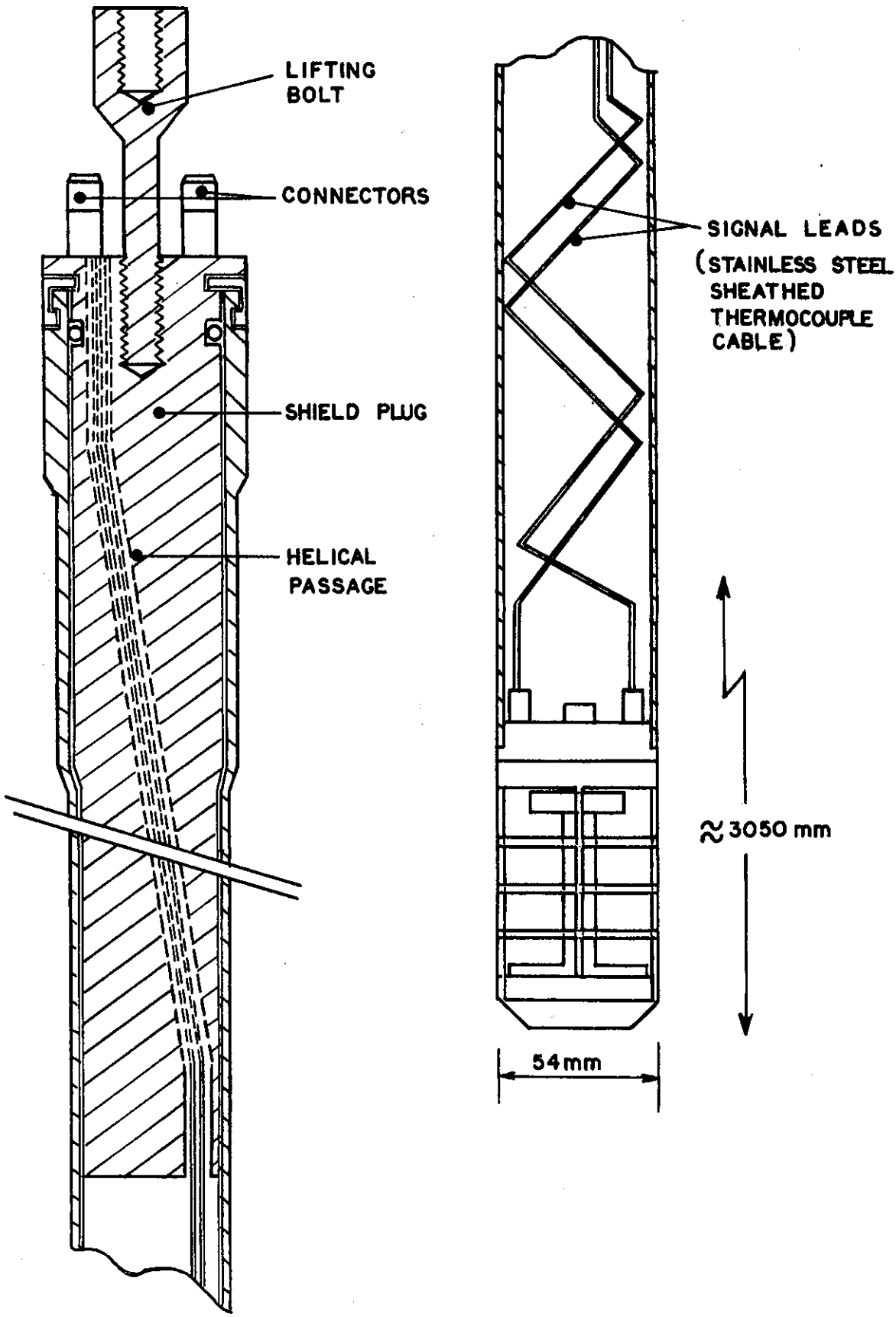

FIGURE 5. DIAGRAMMATIC LAYOUT OF RIG X189

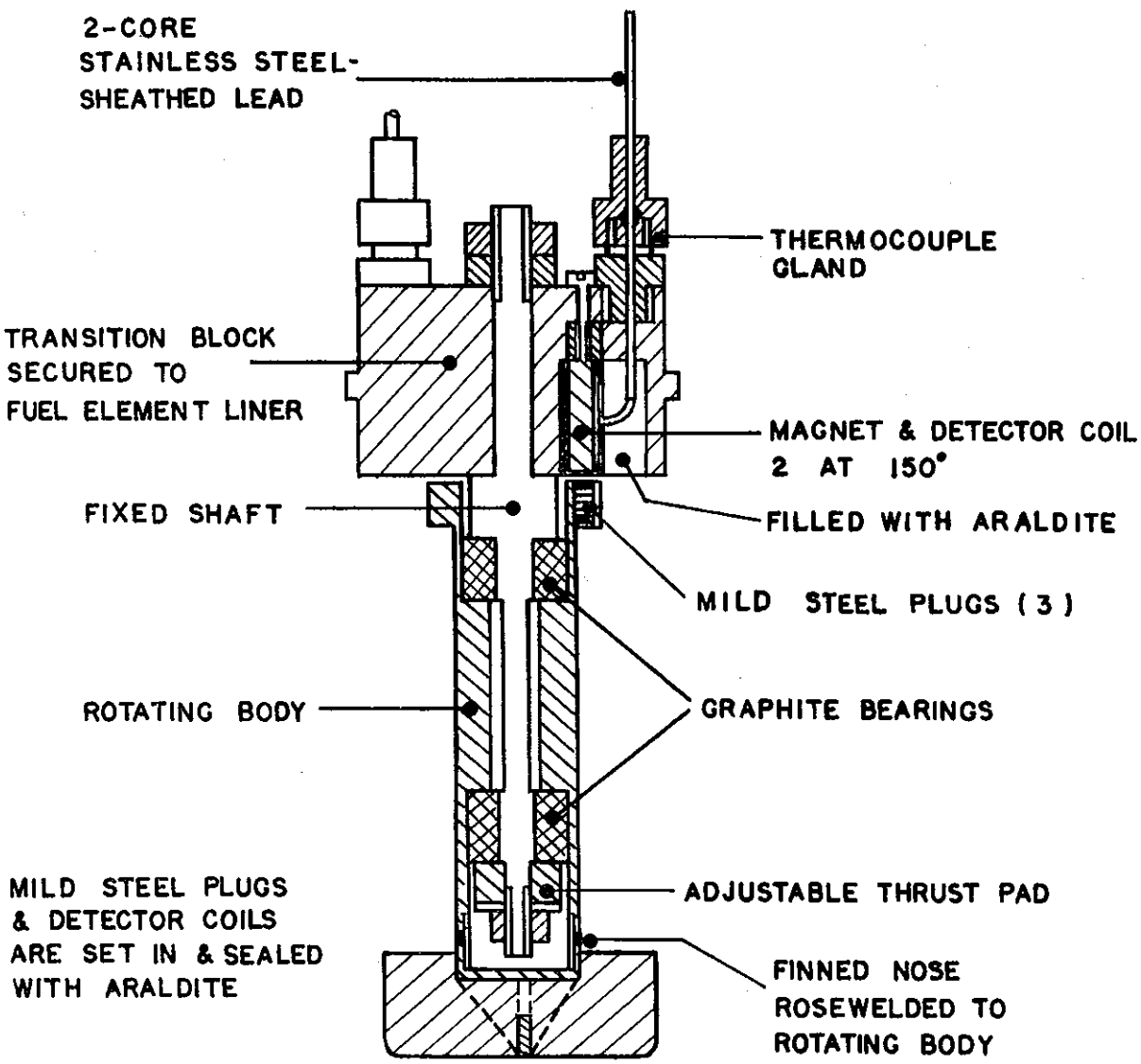

FIGURE 6. VORTICITY METER - CROSS SECTION

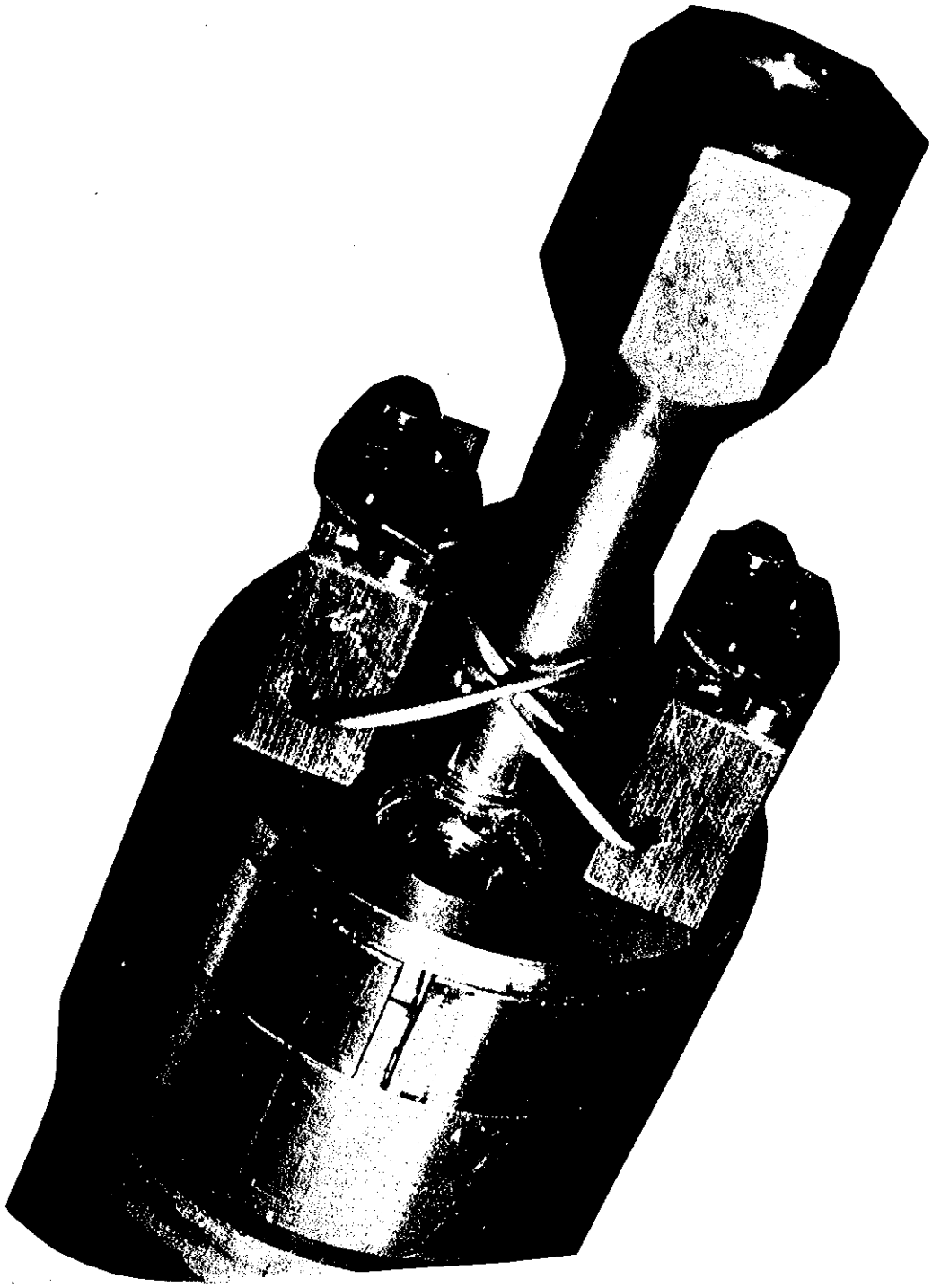

FIGURE 7. END CONNECTIONS

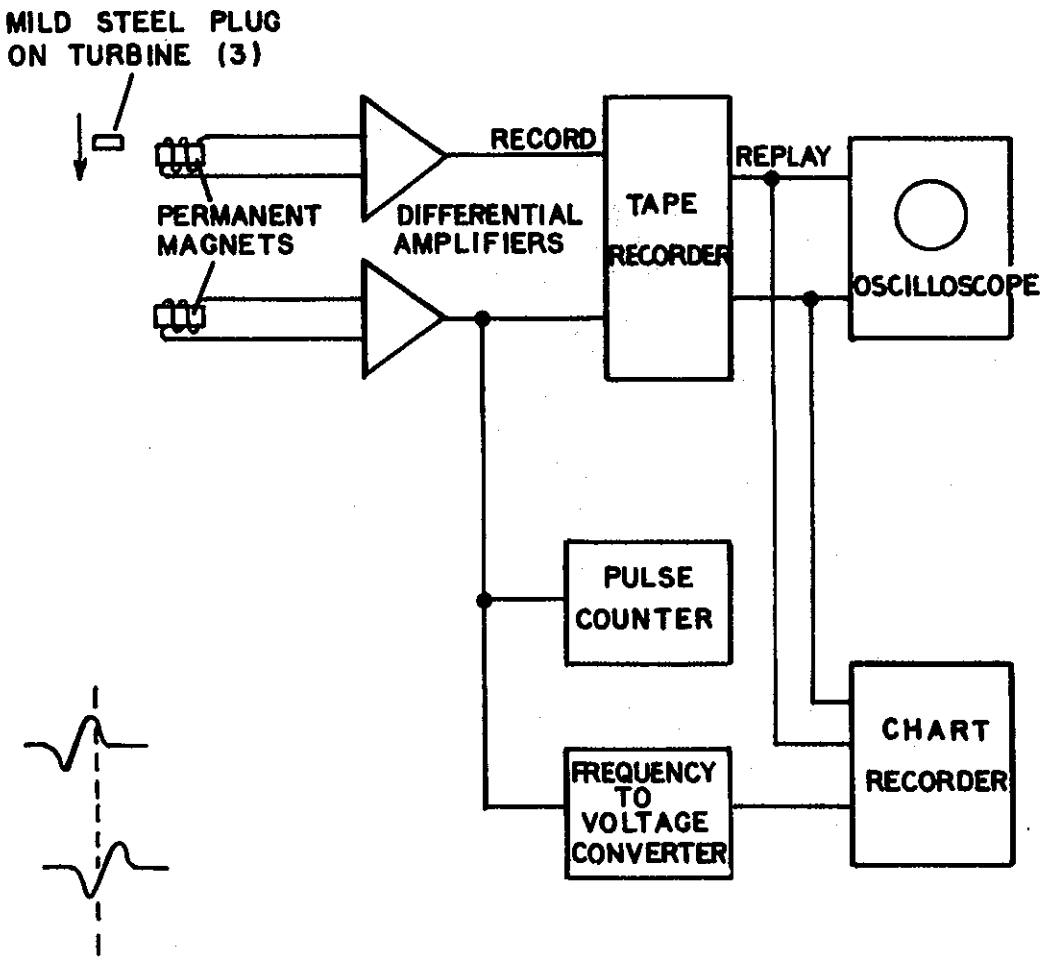

FIGURE 8. RECORDING SYSTEM

POSITION A2 PUMPS 1 & 2

TAPE ER 43 POSITION 48

HIFAR 1st MAY 1973

RECORD GAIN - 200

REPLAY 0·1 v/ DIVISION

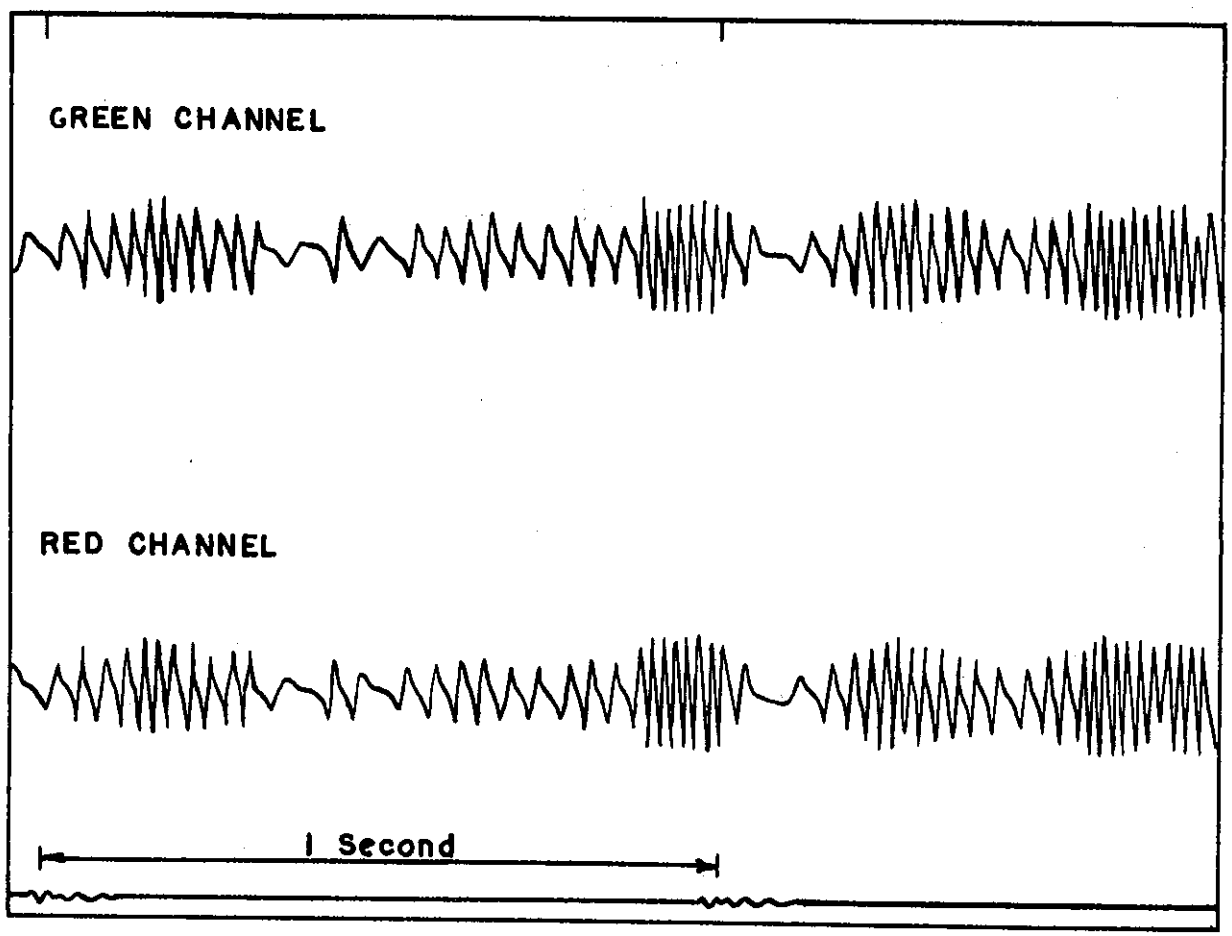

FIGURE 9. LEVEL 1 SIGNALS - POSITION A2

POSITION A3 PUMPS 1 & 2 HIFAR 1st MAY 1973

TAPE ER 43 POSITION 640

RECORD GAIN - 500
REPLAY 0·2 v/DIVISION

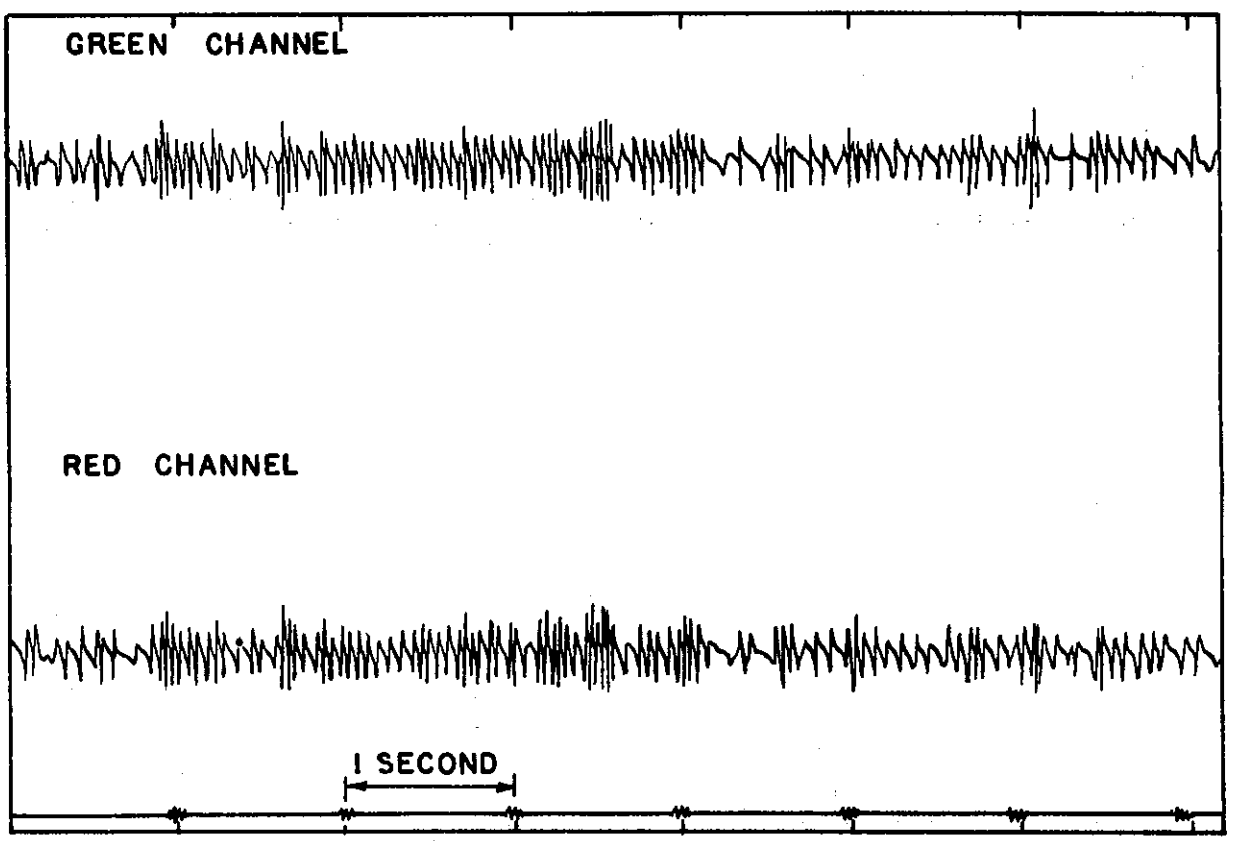

FIGURE 10. LEVEL 2 SIGNALS - POSITION A3

POSITION C3, PUMPS 1 & 2
TAPE ER43, POSITION 375

HIFAR 1st MAY 1973
RECORD GAIN – 500
REPLAY 0·2 v/DIVISION

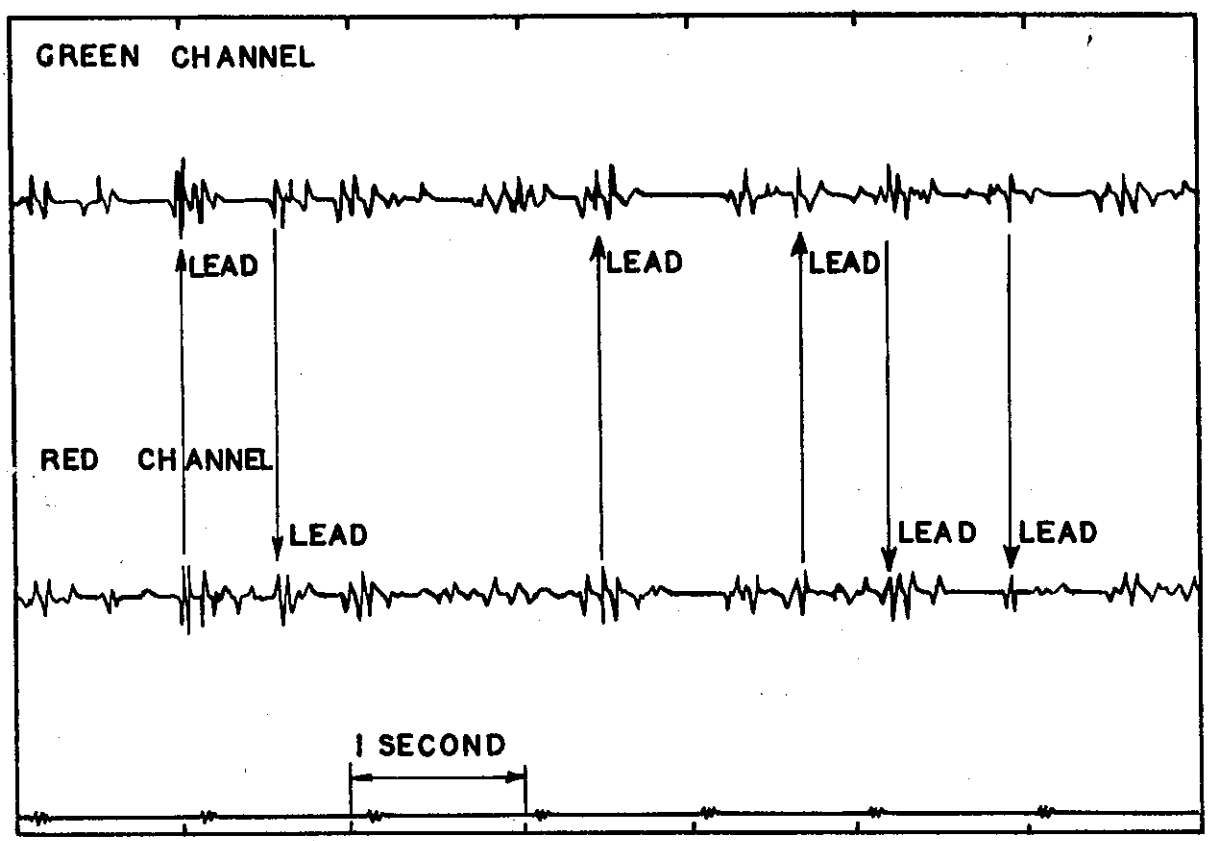

FIGURE 11. LEVEL 3 SIGNALS - POSITION C3

HIFAR 2nd MAY 1974

POSITION D4 PUMPS 1 & 2

RECORD GAIN 1000

TAPE ER 43 POSITION 448

REPLAY 0·5 v/DIVISION

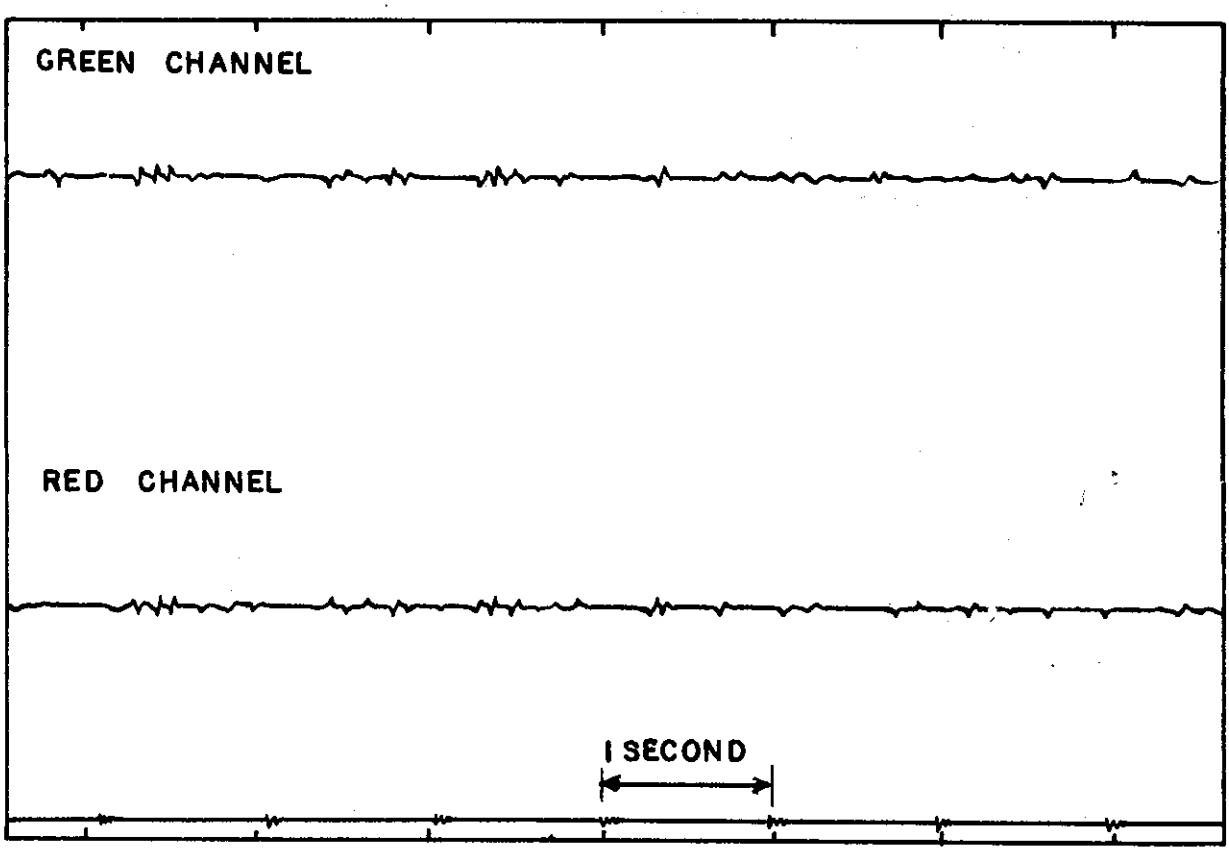

FIGURE 12. LEVEL 4 SIGNALS - POSITION D4

TAPE ER 43 POSITION 675 HIFAR 1st MAY 1973

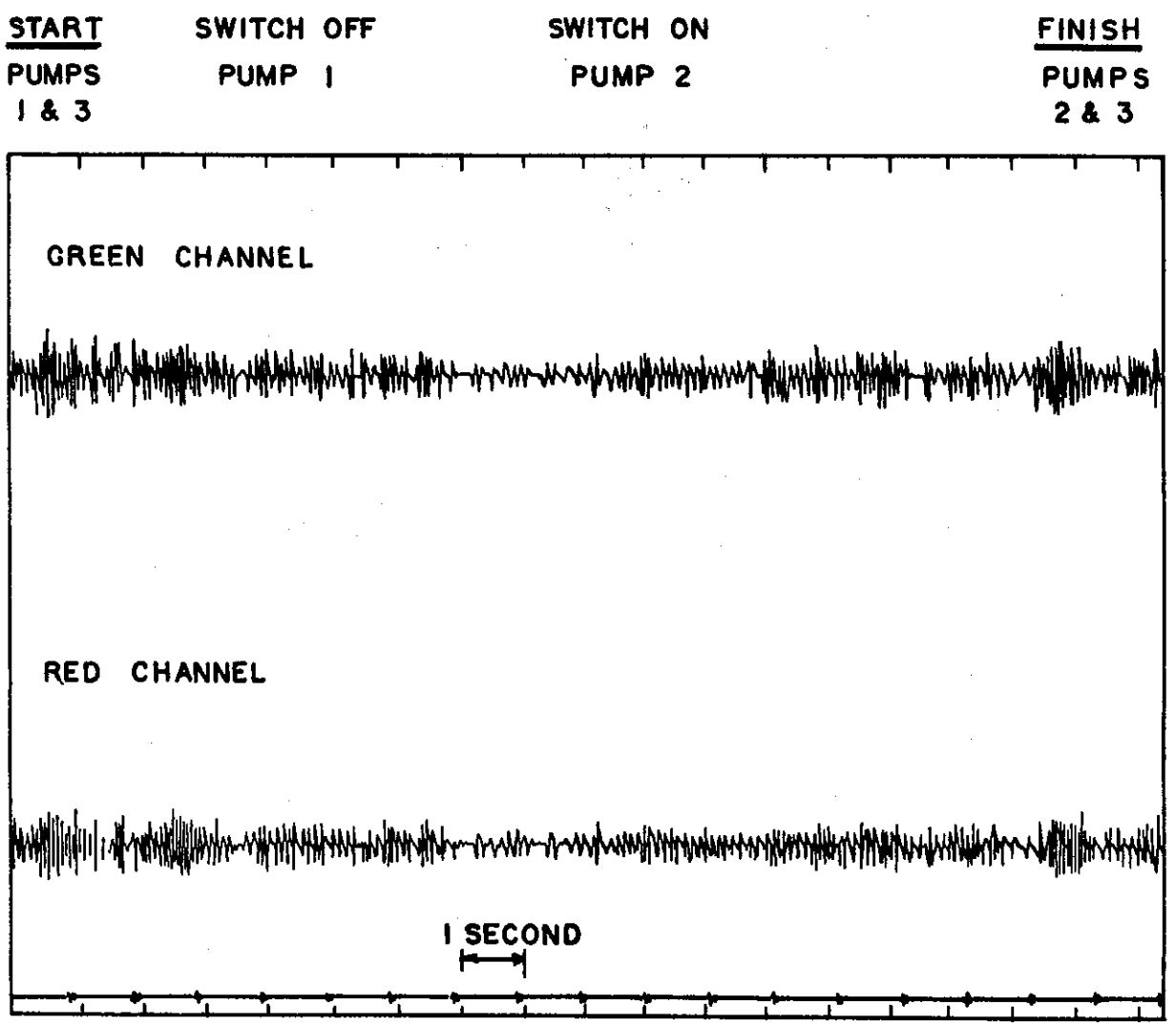

FIGURE 13. PUMP CHANGEOVER - POSITION A3

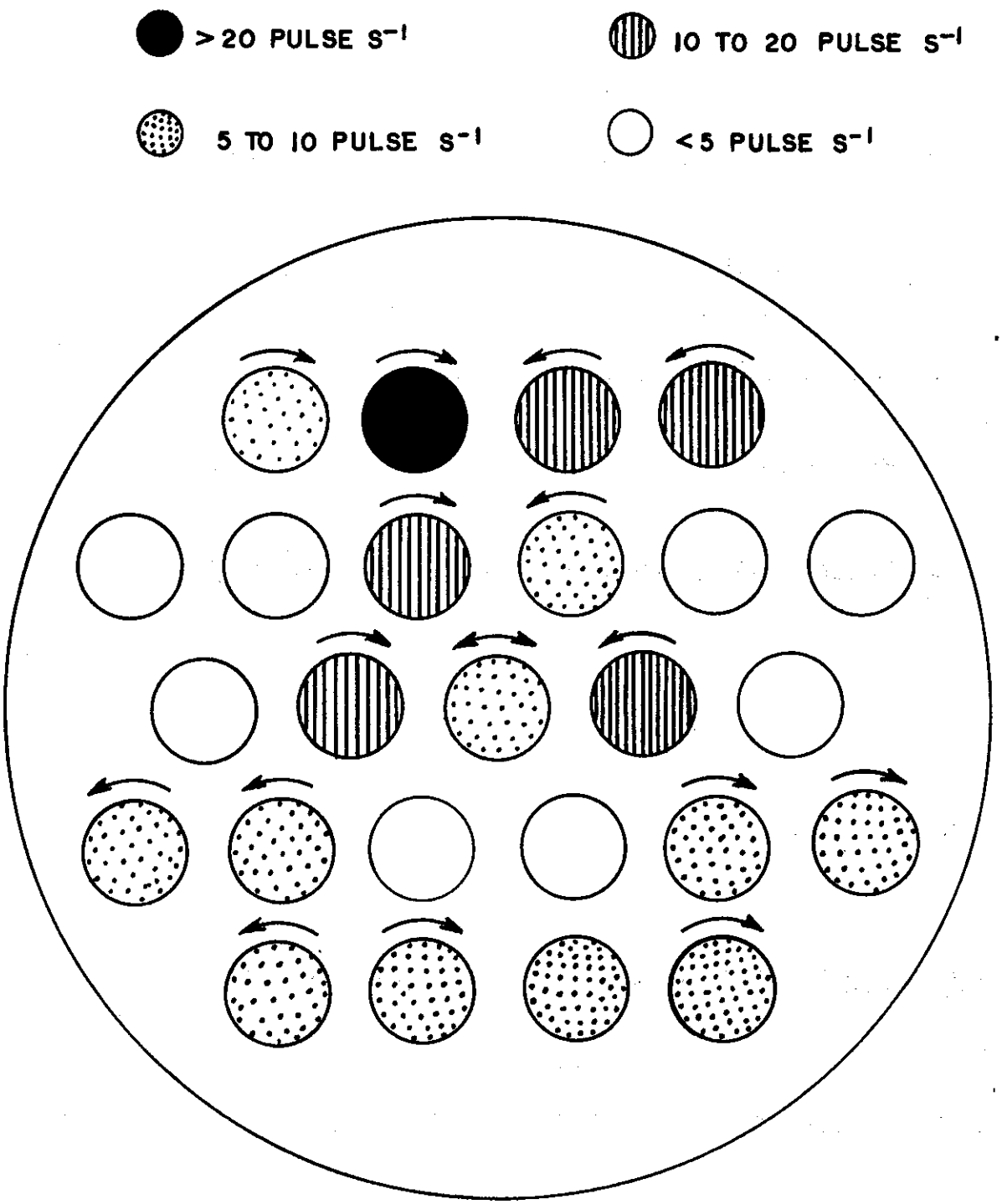

FIGURE 14. DISTRIBUTION OF THE ROTATIONAL ACTIVITY AMPLITUDE AND DIRECTION BEFORE FITTING FLOWSPLITTERS

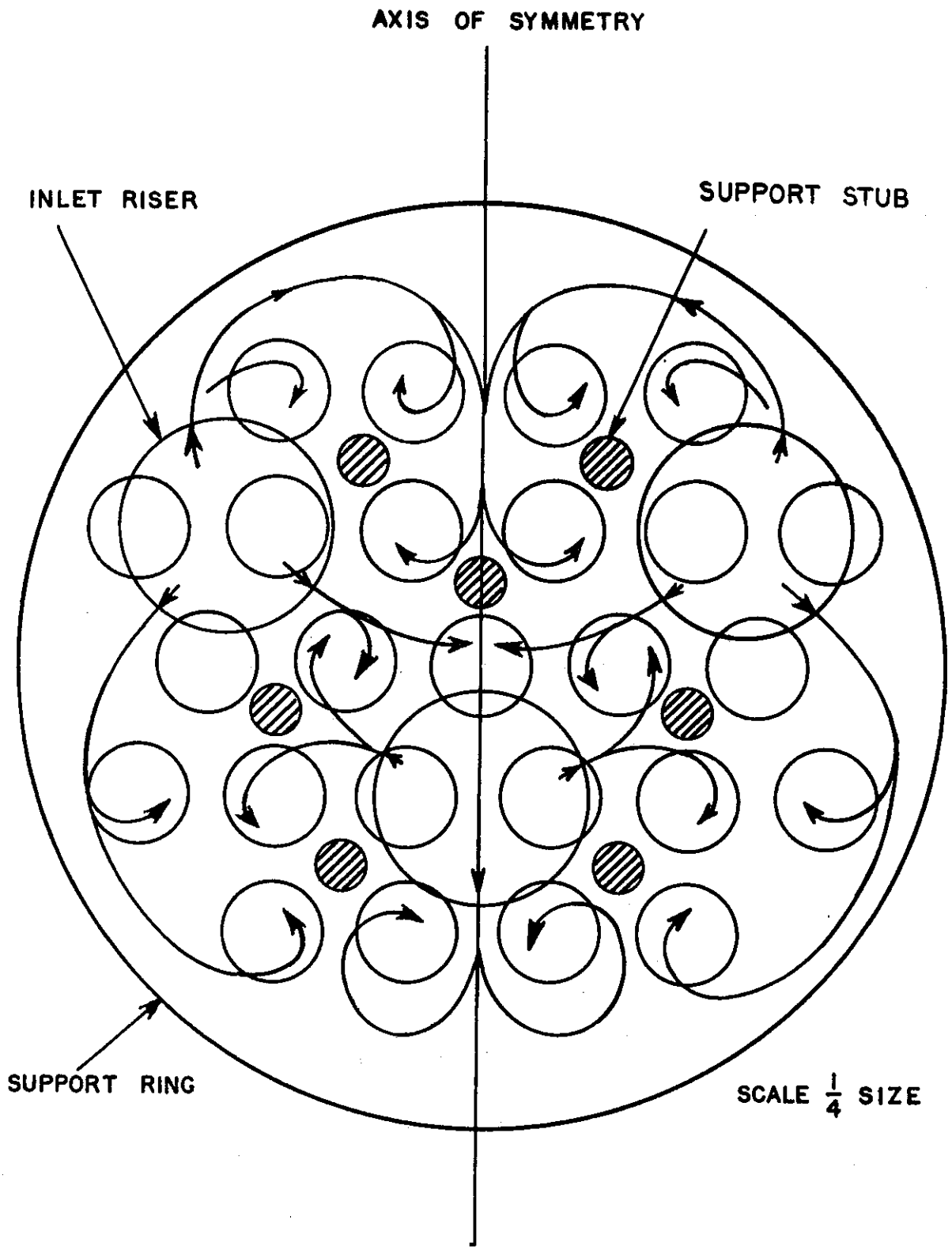

FIGURE 15. POSTULATED FLOW PATTERN IN PLENUM CHAMBER BEFORE FITTING FLOWSPLITTERS

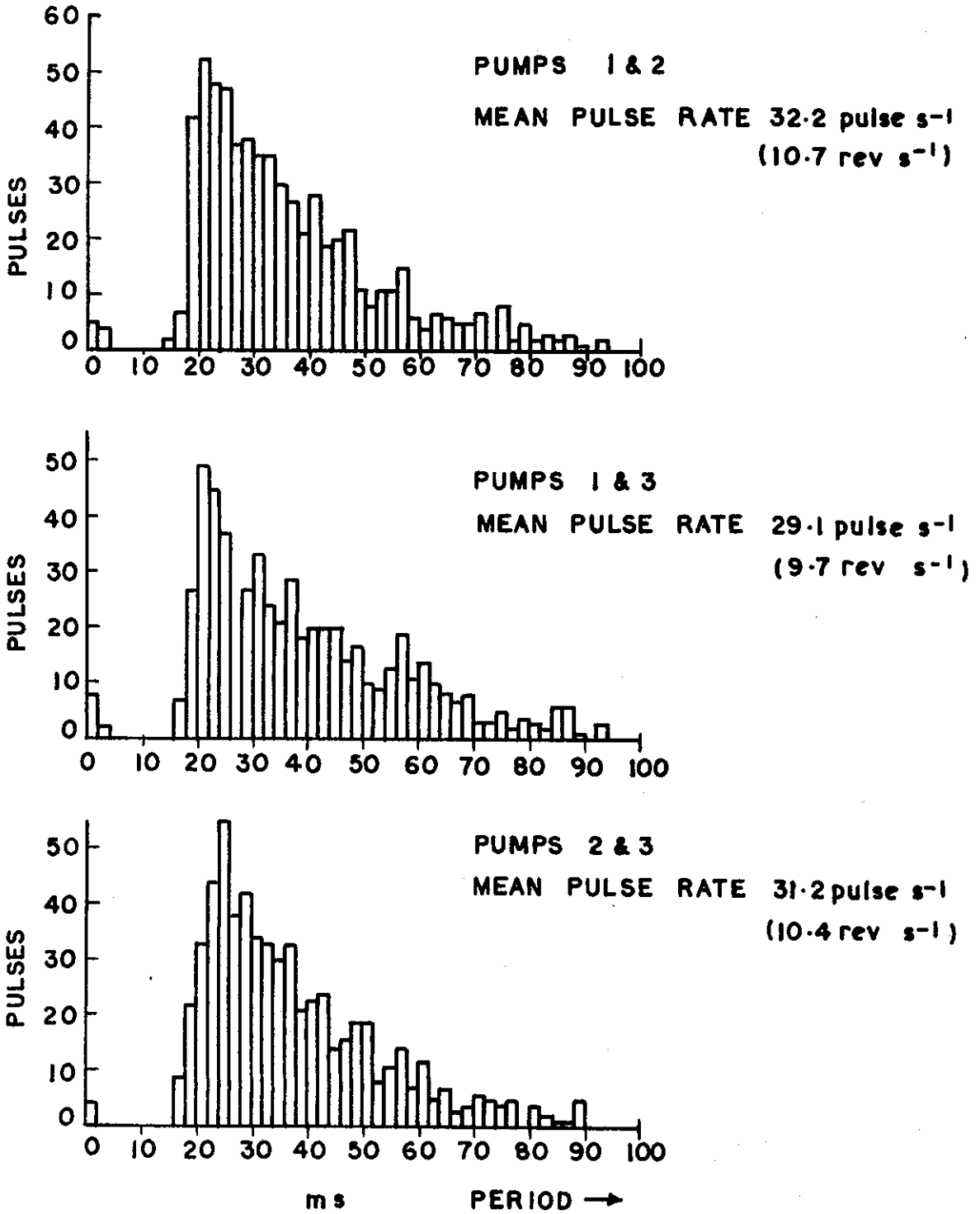

SAMPLE TIME: 20s

FIGURE 16. STATISTICAL DISTRIBUTIONS OF PULSE PERIODS FOR POSITION A2 AT DIFFERENT PUMP COMBINATIONS

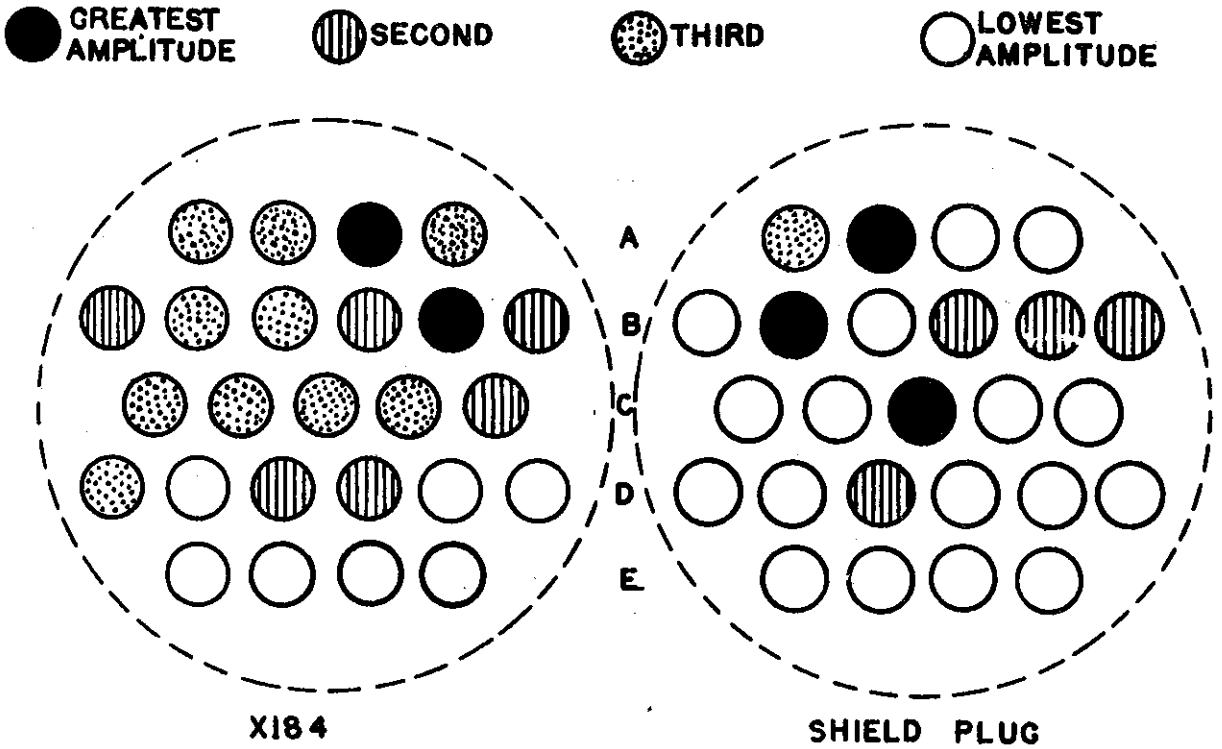

HARRIS & HOLLAND (1974)

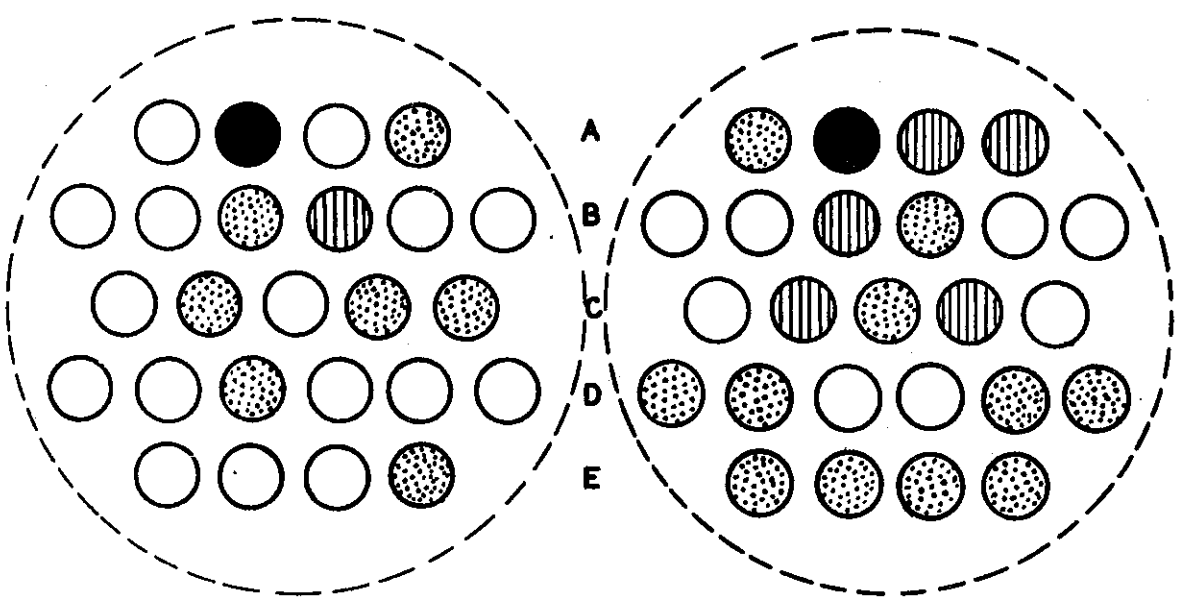

H. MOESKOPS – AAEC PRIVATE COMMUNICATION

FIGURE 17. COMPARISON BETWEEN VIBRATION LEVELS MEASURED AND SWIRL AND FUEL DAMAGE EXPERIENCED

APPENDIX A

EFFECTS OF BEARING FRICTION

An estimation of the minimum rotational velocity detectable by the rig may be made by calculating the moment of forces imposed by the water on the vanes and comparing this with the measured torque required to start the turbine rotating.

The vanes may be considered as thin flat plates in a fluid stream moving at velocity V which, before they move, is inclined at an angle α to the plates. Sabersky, Acosta & Hauptmann (1971) show that, in this situation, the force at right angles to the direction of flow, *i.e.* the lift force per unit length, is

$$\pi \sin \alpha \, \rho V^2 c \quad ,$$

where ρ is the fluid density, and

c is the width of the plate.

In the present case this factor will be considered as acting over a length δr at radius r. If the fluid rotates at constant angular velocity ω, the tangential velocity at r will be ωr, and if the angular velocity is small compared with the linear velocity then

$$\sin \alpha \simeq \frac{\omega r}{V} \quad .$$

Also, if this angle is small then the force may be considered to act perpendicularly to the vanes and the turning moment simultaneously imposed by the fluid on all four blades is

$$M = 4 \Sigma \pi \rho c V \omega r \, \delta r \; r \quad ,$$

which in the limit becomes

$$M = 4 \pi \rho c V \omega \int_{R_1}^{R_2} r^2 \, dr = \frac{4}{3} \pi \rho c V \omega (R_2^3 - R_1^3)$$

$$= K\omega \, ,$$

where $K = \frac{4}{3} \pi \rho c V (R_2^3 - R_1^3)$.

The turbine begins to turn when this moment equals the starting torque of the bearings. Thus, the fluid angular velocity required to start the

turbine rotating is given by

$$\omega_s = \frac{\tau}{K} ,$$

where τ is the measured starting torque (in N m).

Thus, if $\rho = 1{,}050$ kg m^{-3},

$c = 1.9 \times 10^{-2}$ m,

$R_1 = 0.8 \times 10^{-2}$ m,

$R_2 = 2.2 \times 10^{-2}$ m,

$V = 4.9$ m s^{-1},

then $K \simeq 4 \times 10^{-3}$ N m s.

Note that the fluid velocity V was derived by taking the total flow through the fuel channel as 14.5 kg s^{-1} and the channel diameter at the position of the turbine blades as 6 cm.

The starting torque was measured (with a spring balance) at various times during the experiments. In the initial tests the torque was always in the range 16 to 22 g cm. After these tests the rig was slightly active and was kept in a storage facility. On commencing the tests after fitting flowsplitters it was evident that some deterioration had occurred and the starting torque had increased. The turbine was subjected to a running-in period by directing a blast of air onto it and the starting torque then came within the previous range. There was some deterioration again during the August tests and it was decided to dismantle and polish the bearing surfaces after the radiation levels had subsided sufficiently to permit handling. This restored conditions and the starting torque was about 12 to 20 g cm just before the February tests.

The characteristics of this torque were those of dry friction and the running torque, once movement started, was considerably lower than the starting torque. The value when in the reactor and subjected to vibration and turbulence may be much lower than that measured outside. However, taking the starting torque at 2×10^{-3} N m (20 g cm) the water swirl velocity required for starting is

$$\omega_s = \frac{2 \times 10^{-3}}{4 \times 10^{-3}} = 0.5 \text{ rad } s^{-1} = 0.08 \text{ rev } s^{-1} .$$

This value was quite adequate for the initial tests but not very satisfactory for the tests made after fitting the flowsplitters. The types of bearing used were chosen on the basis of the reported experience at Halden (Schenk 1967) with in-core turbine flowmeters, and also because the short

time scale available for the pre-flowsplitter tests made it difficult to obtain other bearings suitable for in-core duty.

APPENDIX B

TIME RESPONSE

If bearing friction is neglected, the time response is governed by the interplay between liquid drag forces and inertial forces according to the equation of motion

$$I \frac{d\omega}{dt} = K (\omega_\ell - \omega) ,$$

where I = the moment of inertia of the turbine about the axis of rotation,

K = the liquid force parameter (Appendix A),

ω_ℓ = the instantaneous liquid angular velocity, and

ω = the instantaneous turbine angular velocity.

The use of the parameter K from Appendix A again supposes that the liquid flow pattern has a high velocity up the channel with a turning, screw-like motion of constant angular velocity about the centre axis.

This equation describes a simple exponential time response to a sudden change in ω, *i.e.* the step function response is

$$\omega = \omega_\ell \left(1 - e^{-\frac{K}{I}t}\right)$$

Here the moment of inertia $I = 1.3 \times 10^{-5}$ kg m^2 and as $K = 4 \times 10^{-3}$ N m s, the time constant $\frac{I}{K}$ is about 3 ms. Thus, the turbine is likely to be able to follow closely any impulse lasting longer than about 10 ms.

APPENDIX C

DAMAGE OBSERVED ON HIFAR MK 4 FUEL ELEMENTS AFTER IRRADIATION AND CROPPING

(H. Moeskops, AAEC private communication)

Fuel Element No.	No. of Programs in Core	Position(s) in Core	Insert	Fuel Tube End Fastening Damage	Rating*
1	1	C5	DR/3	No.1 fuel tube end just slack	3
	5	E4	X169/2		
7	3	C4	X186	Lower tube ends loose	
	2	A4	X175/5		3
10	3	B4	X188	Lower tube ends loose, No.2,3 & 4 tube ends slack at top and No.1 completely free	
	2	A2	FSA/5		2
14	3	B3	FSA/15	No. 2 & 4 lower tube ends just slack	
	2	B3	FSA/6		3
40	5	D3	X95	No.2 & 3 fuel tube ends just slack	3
64	4	C2	X157	No.1 fuel tube end slightly loose on one comb only	3
90	5	A2	FSA/5	No.1 fuel tube ends were loose and fell from top & bottom ends	1

** The ratings are: 1 - worst damage*
2 - moderate damage
3 - slight damage.